V European Conference on Computational Fluid Dynamics
ECCOMAS CFD 2010
J. C. F. Pereira and A. Sequeira (Eds)
Lisbon, Portugal, 14–17 June 2010

STEADY AND UNSTEADY CFD SIMULATIONS OF TRANSONIC TURBINE VANE WAKES WITH TRAILING EDGE COOLING

Gregory M. Laskowski[*] and Frederic N. Felten[†]

[*]GE Global Research Center, Niskayuna NY 12309 USA
laskowsk@research.ge.com

[†]GE Global Research Center, Niskayuna NY 12309 USA
felten@research.ge.com

Key words: Computational Fluid Dynamics, Trailing Edge Wakes, Trailing Edge Cooling

Abstract. *There is an ever-increasing demand for higher performance higher efficiency gas-turbines. The first stage of the high-pressure turbine is subjected to high temperatures as a result. Elaborate cooling strategies are required to ensure the life of the stator and rotor with minimal impact to efficiency. The trailing edges of the vanes and blades that constitute the stator and rotor are particularly vulnerable and coolant flow is typically ejected out the trailing edge to ensure life. This coolant flow interacts with the unsteady trailing edge wake that feeds the downstream blade rows. The present study evaluates RANS and URANS for predicting the downstream momentum and thermal wake evolution. Simulation results for three different trailing edge coolant flow rates are validated against available experimental data. Favorable agreement in vane loading and momentum wake deficits are noted. The URANS simulations capture Kelvin-Helmholtz induced vortex shedding due to the shear layers that form downstream of the suction-side and pressure-side surfaces. Resolving the resulting vortex shedding is shown to have a small impact on the wake evolution. It is shown that the momentum and thermal wakes evolve in different locations that are attributed to compressibility, shock formation and coolant ejection location.*

1 INTRODUCTION

Gas turbine technology continues to evolve to meet demands for higher efficiency. One of the primary drivers for improved efficiency is the firing temperature of the combustor. Higher temperatures, coupled with higher compressor pressure ratios, can improve the overall efficiency of the engine (Wilcock et al., 2005). Higher combustor temperatures require intricate cooling strategies in the downstream turbine to ensure turbine component life (Bunker, 2007). This is typically accomplished by utilizing high temperature metal alloys and coatings in the construction of turbine components and by diverting a certain potion of air from the compressor, bypassing the combustor, and circulating it through internal cavities of the vanes and blades for coolant purposes. A significant portion of this coolant flow is blown out the trailing edge (TE) for convective cooling purposes. Understanding the impact of this coolant flow on mixing losses and wake evolution is essential in understanding stage performance and wake impact on downstream blade rows. This paper focuses on a fundamental numerical study of a transonic vane with trailing edge cooling to understand the impact of the coolant flow on wake evolution and migration.

Unsteady flow behind bluff bodies has received significant attention by the scientific community. Roshko (1954) presents an excellent overview on the differences between large-scale unsteadiness and turbulence for flow past a circular cylinder at different Reynolds numbers. Measurements of downstream streamwise-velocity components were conducted. For low Reynolds numbers the energy content of the flow downstream is comprised of large-scale deterministic unsteadiness. At increasingly higher Reynolds numbers the energy content will contain added contributions from turbulent random fluctuations. More recently, Williamson (1996) provided a review of the dynamics in wakes for laminar, transitional and turbulent flow and 3D instabilities.

A significant amount of work has been done regarding unsteady effects of trailing edge cooling on trailing edge heat transfer (Martini et al., 2006; Medic and Durbin, 2005) as well as un-cooled trailing-edge wakes.

Sieverding and Heinemann (1990) demonstrated experimentally that the fundamental frequency of large-scale vortex shedding downstream of a 2D transonic turbine airfoil is a strong function of the boundary layer state. The Strouhal number changed by nearly 80% based of the boundary layer that formed the shear layers on the suction-side and pressure-side surfaces at the trailing edge. Gehrer et al. (2000) further demonstrated that the shedding frequency of an un-cooled turbine vane was a strong function of the trailing edge shape and Reynolds number based on linear cascade data. Cicatelli and Sieverding (1997) investigated the impact of unsteady vortex shedding on the pressure-side and suction-side surfaces in the vicinity of a thick trailing edge without trailing edge cooling. The pressure fluctuations impacted the boundary layer flow developing on the pressure-side and suction-side surfaces approaching the trailing edge. The Root Mean Square (RMS) values of the fluctuations were dominated by the periodic component with a smaller contribution coming from the random component. Later, Sieverding et al. (2003) attributed strong suction-side pressure variations to downstream vortex shedding.

The studies noted to this point have not considered trailing edge cooling impacts on downstream wakes. Brundage et al. (2007) presented trailing edge heat transfer and downstream aerodynamic wake measurements of a flat plate model with different 3D ejection geometries and coolant mass flow ratios. Optimal coolant flow rates for heat transfer and aerodynamics were noted for 2.8% and 2.1% respectively. Ames et al.

(2007) demonstrated a strong relation between Reynolds number, free-stream turbulence, and blowing rate on aerodynamic losses for a 2D vane linear cascade with 3D ejection geometries. Chen et al. (2008) conducted 2D PIV measurements downstream of a NACA 0012 airfoil with pressure-side bleed slots. Velocity and turbulence measurements were made for different blowing rates. The measurements demonstrate impact of a 3D slot geometry on energy exchange between different velocity components. Kapteijn et al. (1996) conducted an experimental investigation of pressure-side and trailing-edge cooling ejection geometries of a 2D transonic vane in a linear cascade. This work was done in conjunction with the work of Sieverding et al. (1996) who conducted a similar investigation for the same airfoil radially stacked in an annular cascade. Both investigations considered air as the coolant flow and measured downstream total pressure (1D profiles by Kapteijn et al. and 2D planar contours by Sieverding et al.). Kapteijn et al. also conducted simulations with CO_2 as the coolant flow to study density ratio effects as well as to assess the concentration wake evolution. The present study investigates the predictive capability of steady and unsteady Reynolds Averaged Navier Stokes (RANS and URANS respectively) for the momentum and concentration wakes reported experimentally by Kapteijn et al. for different blowing rates. The goal is to better understand the role of unsteadiness on the downstream total pressure and concentration wake evolution and mixing.

2 OVERVIEW OF CASE FOR NUMERICAL STUDY

The pressure-side cooling configuration of Kapteijn et al. (1996) was selected for the present study and the vane geometry is provided in Table 1.

Table 1. Vane geometry details (from Kapteijn et al., 1996).

Isentropic outlet Mach No.	$M_{2,is} = 1.05$
Outlet Re_2	$Re_2 = 10^6$
Outlet flow angle	$\alpha_2 = 70\ldots75°$
Pitch-to-chord ratio	g/c = 0.75
Chord length	c = 72.00 mm
Axial chord length	c_{ax} = 43.10 mm
Stagger angle	$\gamma = 51.9°$
Trailing edge thickness	te = 1.70 mm

The primary flow was air with total pressure $P_t = 1.62x10^6$ Pa and total temperature T_t = 440 K. The turbulence intensity was quoted TI = 1%. Studies were conducted for both air and CO_2 as the secondary flow at a temperature of T = 287 K and for secondary to primary mass flow ratios of cm = 0%, 2%, 3% and 4%. Downstream mixing between the two gases was assumed to be dominated by turbulent mixing and not diffusion so the diffusion coefficient was set to a small value. The validation metrics consisted of vane loading, wake total pressure profiles and characterization of CO_2 in the wake.

3 COMPUTATIONAL DETAILS

Three-dimensional simulations were conducted using CFX v11.0. A two fluid problem was simulated in order to be consistent with the experiment. The hot gas path flow was assumed to be air with R = 287 J/kg K and γ = 1.40 whereas the secondary coolant flow was assumed to be CO_2 with R = 189 J/kg K and γ = 1.28. This approach

enabled accurate treatment of the local gas thermodynamics which thus ensured the CFD matched the experimental density and momentum ratios for the ejected flow.

Figure 1 presents the computational domain and boundary conditions. A single vane was simulated with translationally periodic boundary conditions specified at mid-pitch to mimic conditions of a linear cascade. Total pressure and temperature were specified at the inflow boundary consistent with those reported. The static pressure was set at the outflow boundary based on the pressure ratio of the experiments. Adiabatic wall boundary conditions were assumed for all of the vane surfaces and sidewalls. Subsequent simulations replaced the sidewalls with periodic boundary conditions as the aspect ratio was deemed sufficiently large so that the midspan flow was essentially 2D and not impacted by secondary flow structures near the sidewalls. This reduced the computational cost of the simulations. Finally, the secondary flow mass flow and temperature were prescribed at the location shown in Figures 1 and 2.

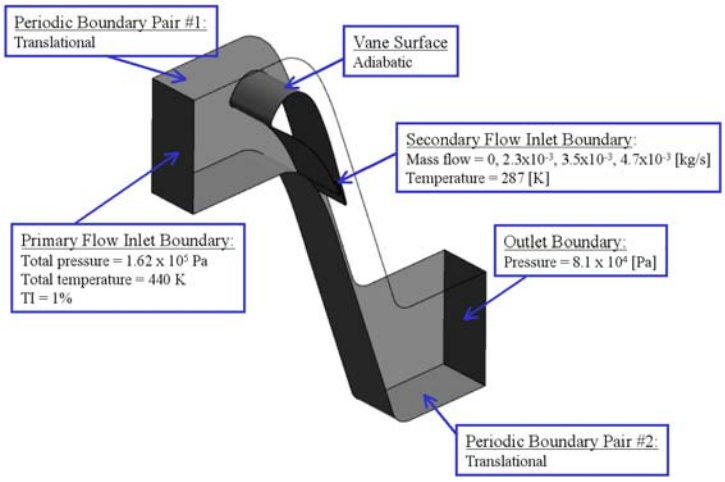

Figure 1. Computational domain and boundary conditions.

The computational grid consisted of tetrahedral elements in the core flow and prism elements near the solid walls to resolve the boundary layer as shown in Figure 2. The grid was constructed such that 20 prism elements spanned the boundary layer with a near wall spacing that ensured $\Delta y^+ < 1$ everywhere. Mesh sensitivity studies were conducted for the wake and boundary layer flows. No attempts were made to resolve the passage shock. It was determined that local refinement was needed in the slot region and in the wake to achieve grid independence. Additional refinement was added up to one chord downstream, the approximate location of a downstream bladerow, and depicted in Figure 2. This resulted in nearly 150 control volumes spanning the lateral extent of the unsteady wake and nearly half of which resolved the resulting time averaged wake. It is important to note that this high level of refinement exists for profile locations 1 and 2 but not for locations 3 and 4.

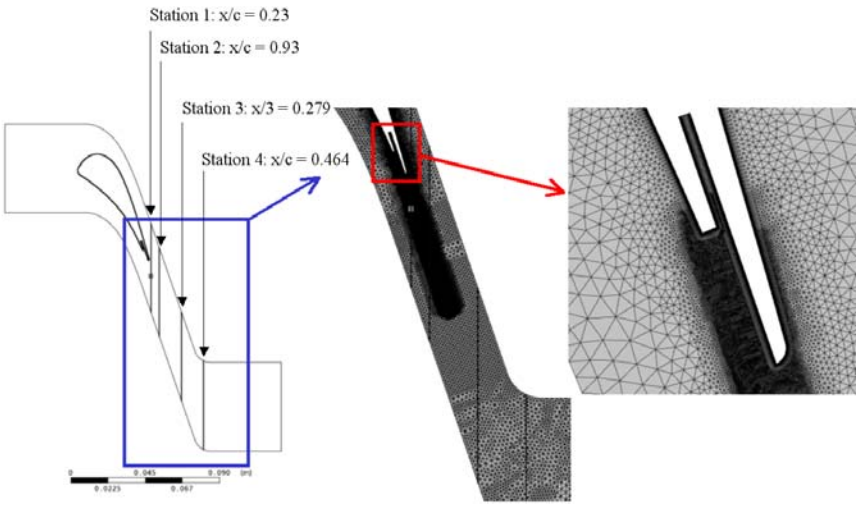

Figure 2. Coolant ejection geometry, wake profile locations and computational grid.

An assessment of turbulence models was performed for the cm = 3% design point. Steady RANS simulations were conducted with the k-ω (Wilcox, 1988), SST (Menter, 1994) and Spalart-Allmaras (Spalart and Allmaras, 1992) turbulence models. Both RANS and URANS calculations were conducted with the Wilcox k-ω turbulence model only. All simulations were conducted with a constant turbulent Prandtl number Pr_T = 0.9 which is questionable for wake evolution with heat transfer and turbulent mixing (Xu and Zhou, 2005). The RANS simulations were considered converged when all equation RMS residuals reached at least $1.0x10^{-6}$. The URANS simulations were conducted with a time step of $\Delta t = 5.0x10^{-7}$ seconds with 5 inner iterations to converge each time step. The unsteady simulations were initiated from the steady simulations and advanced in time until a statistical steady state was achieved. The time step used for the simulations resulted in approximately 35-40 time steps per shedding cycle. Time averaging took place over 12 shedding cycles.

4 RESULTS

Figure 3 compares experimental and numerical Schileren images of the passage shocks and downstream wake for the cm = 3%. The oblique shock that forms off of the pressure-side bleed slot impacts the suction-side surface of the neighboring blade. Shock induced boundary layer separation on the suction-side surface was noted by the experimental Schlieren and was predicted in the CFD case for the cm = 0% case. CFD simulations for cm = 2% and higher did not show boundary layer separation. The flow continues to accelerate and ends in a strong normal shock sitting on the trailing edge suction-side surface.

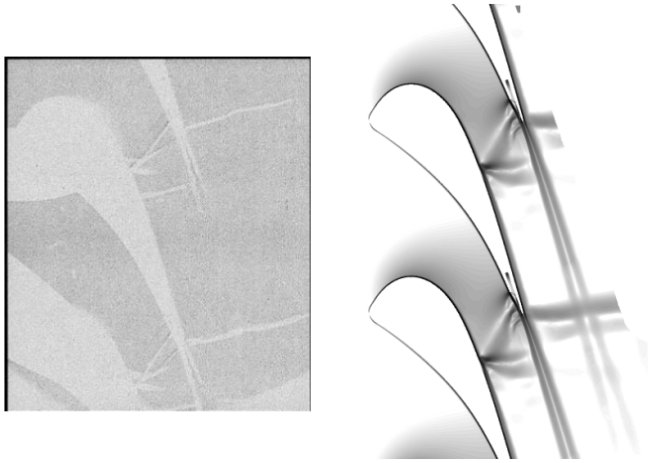

(a) (b)

Figure 3. Schlieren visualization for cm = 0%
(a) From Kapteijn et al (1996) [reproduced by permission ASME] (b) Numerical Schlieren (steady, k-ω)

Figure 4 presents vane loading RANS results for different turbulence models at the design cooling flow case cm = 3%. Also included in the figure are results for time averaged k-ω URANS and compares the impact of blowing air and CO_2 through the slot. The impact of turbulence models on vane loading, even in the vicinity of the shock-boundary layer interaction location near x/c = 0.3, is negligible. Furthermore, the impact of blowing air versus CO_2 has no discernable impact on vane loading. The only notable difference is the comparison of RANS and URANS. The time averaged URANS results are in closer agreement with the shock strength but predict a throat location that is slightly further downstream than was measured experimentally.

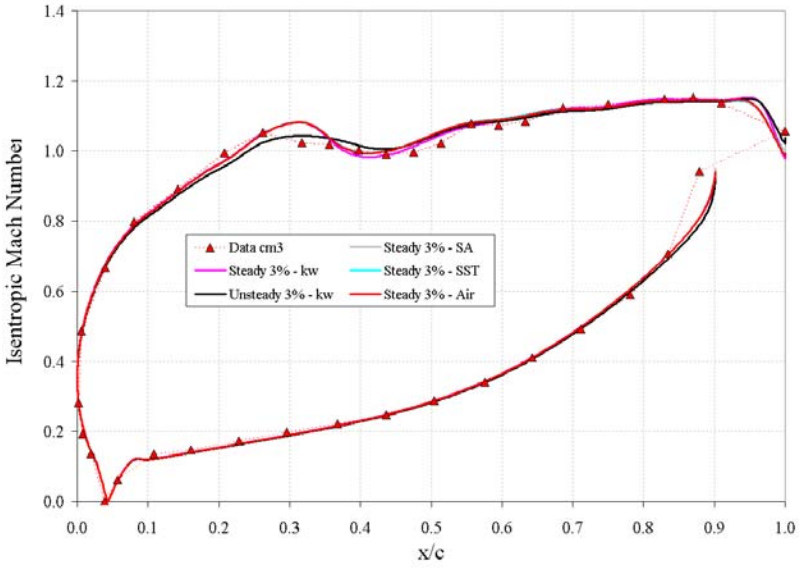

Figure 4. Vane loading for different scenarios (cm = 3%)

Figure 5 presents steady k-ω RANS computed Mach number contours in the cascade for the four blowing rates considered in this investigation. The case with no blowing effectively results in a backward-facing step on the pressure-side surface at the slot breakout location. The result is a strong normal shock in the passage. The addition of

cooling flow acts as a streamline for the primary flow and reduces the shock strength. Further increasing the coolant supply effectively reduces the passage area and reduces the strength of the passage shock that forms off of the pressure-side surface just upstream of the coolant discharge location.

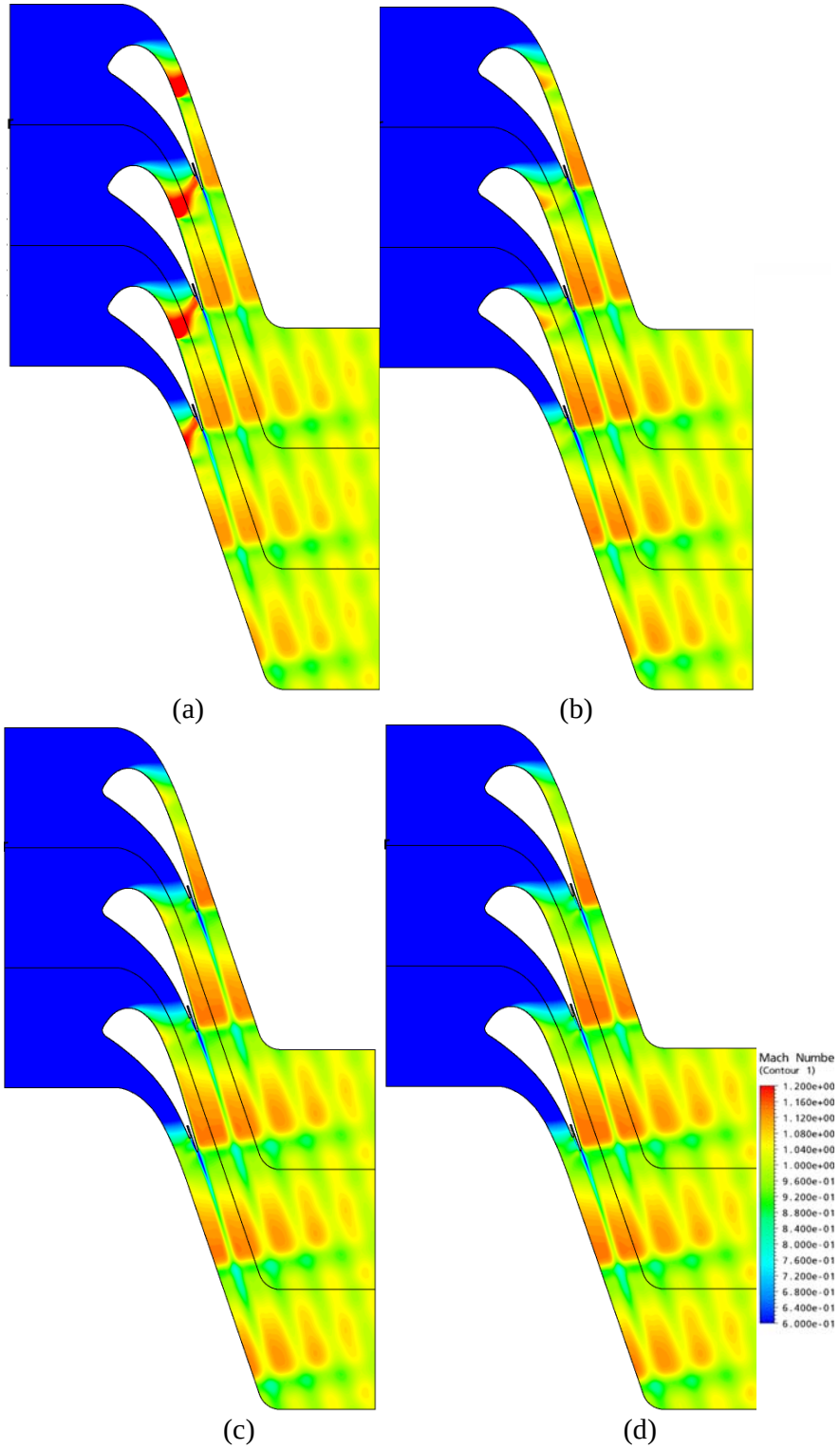

Figure 5. Mach number contours for different coolant flow rates (steady, k-ω)
(a) 0% (b) 2% (c) 3% (d) 4%

Figure 6 shows the steady k-ω RANS computed surface isentropic Mach number distribution on the pressure-side and suction-side surfaces plotted against the experimental data for different secondary flow rates. Aside from the noticeable differences at the shock location near x/c = 0.4 the agreement is comparable. Increasing the amount of coolant flow ejected through the trailing edge impacts the loading on the suction-side in two ways. First, it causes the throat location (M = 1) to shift downstream slightly as can be seen near x/c = 0.2. Second, and far more noticeable, the shock strength weakens with increased coolant flow rate due to displacement effects. The pressure recovery downstream of the shock (0.5 < x/c < 1.0) is a strong function of no-flow vs flow cases but is independent of the amount of coolant flow ejected.

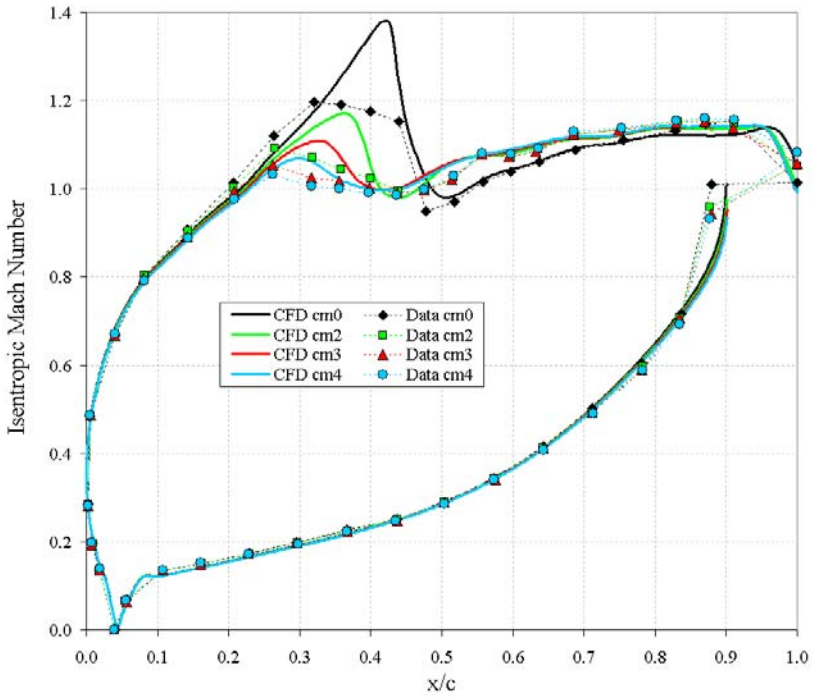

Figure 6. Surface isentropic Mach number distributions along vane pressure-side and suction-side surfaces along mid-span (steady, k-ω).

All subsequent results are for simulations with CO_2 as the secondary flow. The impact of large-scale unsteadiness on the wake can be seen in Figure 7. The instantaneous span-wise vorticity in the wake shows the impact of the Kelvin-Helmholtz induced vortex shedding for the cm = 3% case. The computed Strouhal number for this shedding was determined to be St = 0.277 based on downstream average velocity and trailing edge radius (Table 1) of the original airfoil. This finding is comparable with those of Ning and He (2001) who conducted URANS simulations for an un-cooled transonic vane with a thick trailing edge measured experimentally by Cicatelli and Sieverding (1997). Ning and He (2001) reported URANS predictions of St = 0.245 whereas Cicatelli and Sieverding (1997) reported an experimentally measured value of St = 0.27.

Figure 7. URANS instantaneous span-wise vorticity for 3% case (unsteady, k-ω)

Figure 8 shows the extent of the thermal wake for cm = 3%. The impact of the trailing edge vortex shedding is clearly evident on the thermal wake. However, the time averaged wake is qualitatively similar to the steady wake. This will be quantified in more detail later.

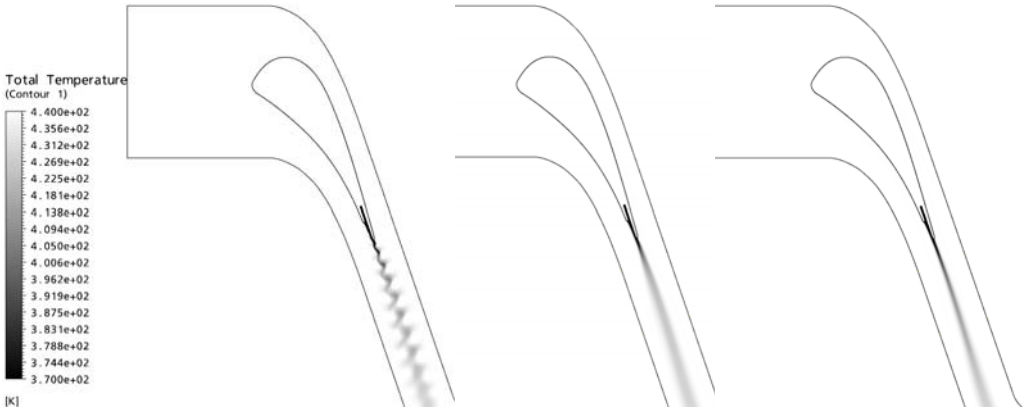

Figure 8. Total temperature contours in wake for cm = 3%
(a) k-ω URANS: Time instantaneous (b) k-ωURANS: time averaged (c) k-ω RANS

In order to better understand the time-scales associated with the unsteadiness and turbulent mixing an assessment of large-scale structures (integral scale)

$$\tau_L = k/\varepsilon \qquad \textbf{Eq (1)}$$

and small-scale structures (Kolmogorov scale)

$$\tau_\eta = (\nu/\varepsilon)^{1/2} \qquad \textbf{Eq (2)}$$

based on the steady RANS results were computed and are presented in Figure 9. The integral time scale computed is precisely the range of the vortex shedding time scale of $\tau = 1.75 \times 10^{-5}$ seconds discussed earlier.

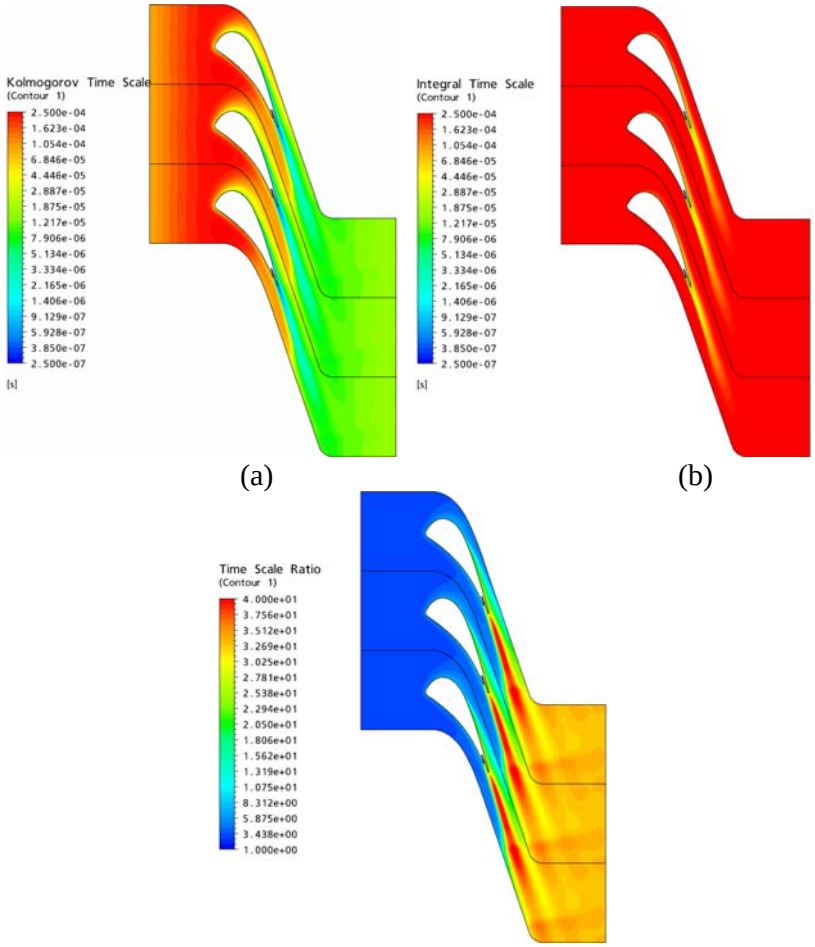

Figure 9. Time scales for cm = 3% case (a) Kolmogorov time scale (log scale) (b) Integral time scale (log scale) (c) Time scale ratio (linear scale)

Figure 10 compares steady RANS results for different turbulence model predictions of the thermal and momentum wakes. Both the total pressure and total temperatures are normalized by the free-stream value for Station 1. The impact of the different turbulence models is relatively benign and has seemingly no impact on wake evolution or mixing. Initially the thermal and momentum wakes are aligned along different axes as shown at Station 1. This misalignment can be attributed to the shocks and viscous losses responsible for a large total pressure wake. In the absence of cooling these mechanisms have a minor impact on the thermal wake. Introducing cooling through the pressure-side bleed slots results in a thermal wake directed along the axis of ejection which is different than the momentum wake which is largely dominated by shock and viscous losses.

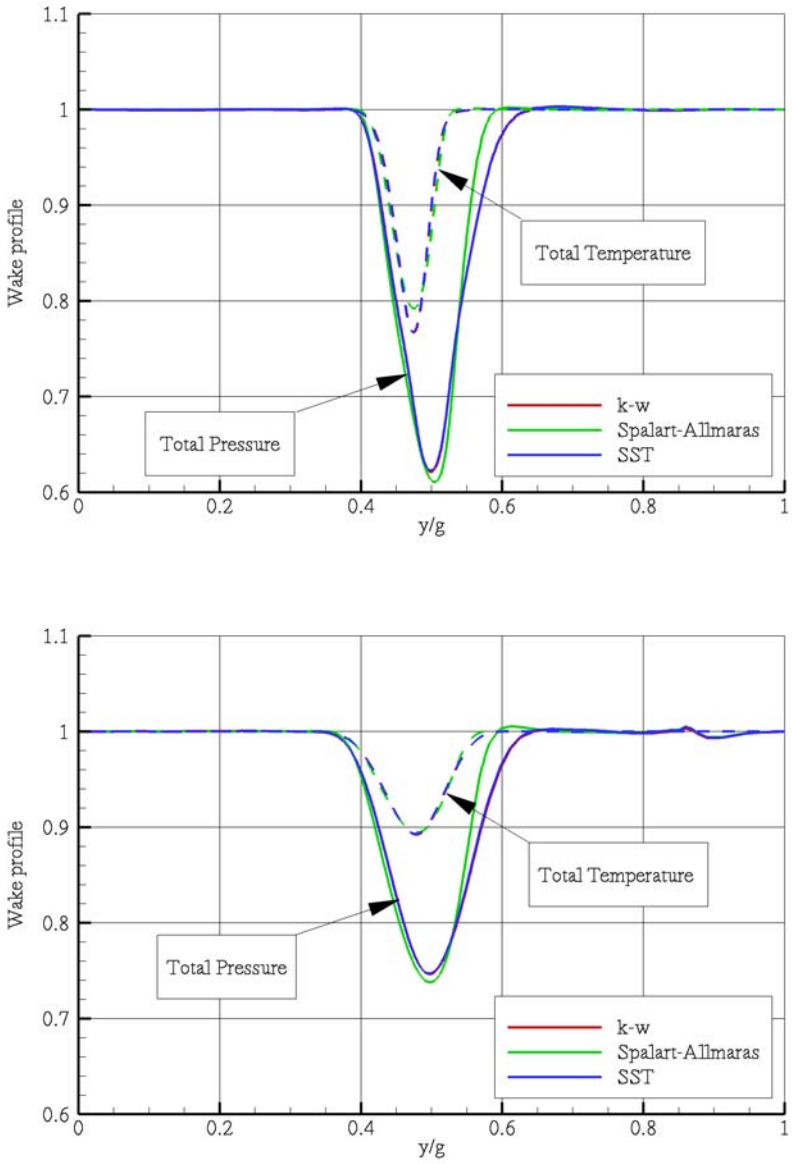

Figure 10. Momentum and thermal wake predictions for different turbulence models: Station 1 (upper) and Station 2 (lower).

Comparison against available data for the momentum wake is provided in Figure 11. Unfortunately no data is available to directly validate the thermal wake predictions. The figure shows k-ω RANS and time-averaged URANS predictions in the wake compared against available experimental total pressure measurements for cm = 3% at the locations shown in Figure 2. Initially the momentum wake prediction is too deep which can be attributed to insufficient lateral mixing in near the shear layer. The wake mixes out rapidly as it progresses from Stations 1-4. It should be noted that Station 1-2 are in wake regions with a highly refined mesh, which is intended to resolve the wake, whereas Stations 3-4 resort back to a nominal grid spacing. The coarse mesh tends to increase the numerical dissipation and enhances the lateral mixing not provided by the turbulence model or vortex shedding.

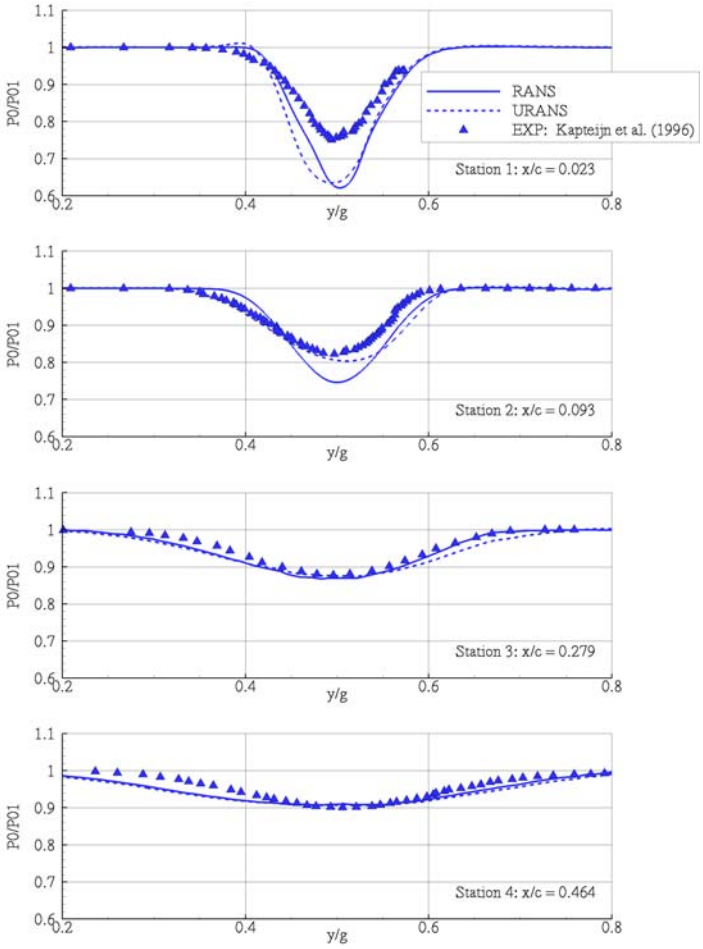

Figure 11. Vane wake total pressure profiles at Stations 1-4 in wake for cm = 3% case.

Figure 12 presents the momentum and thermal wake evolution for the RANS and time-averaged URANS simulations. The simulations suggest that on the fine mesh the impact of the vortex shedding is to make the wake wider and more consistent with the experimental data. However as the wake propagates downstream from the highly resolved mesh to the much coarser mesh the agreement with the experimental data improves. Again, this is attributed to numerical dissipation on the fine mesh that enhances the dissipation in the transverse direction across the shear layer. The turbulence models do not adequately capture the lateral mixing that is required to match the experimentally derived wake evolution. Furthermore, as noted earlier, the thermal and momentum wake evolution apparently evolve along different axes with respect to the vane ejection point. This could prove significant for more realistic vane cooling configurations that include a passage vortex, film cooling and discrete diffusion-shaped ejection slots that would introduce streamwise vorticity.

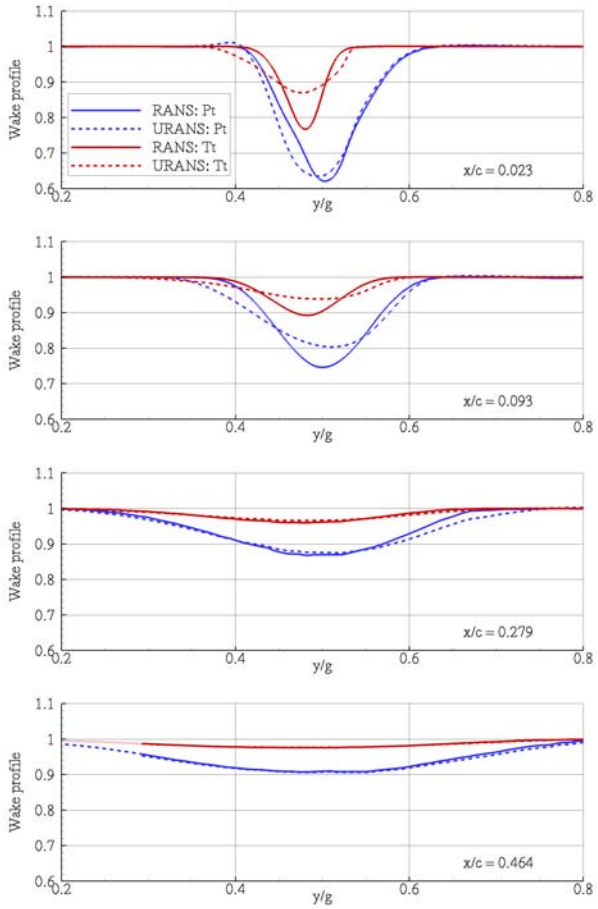

Figure 12. Vane wake total pressure and total temperature Stations 1-4 wake profiles for cm = 3% case (k-ω RANS and URANS)

The rate at which the temperature wake mixes out can be approximated by the CO_2 distribution in the field, barring compressibility effects which are significant for this transonic vane simulation. Regardless, Figure 13 presents maximum CO_2 concentration at the different station locations. It is clear that the steady RANS simulations on the highly refined mesh mix out at a far slower rate than is demonstrated by the experimental data and suggested by the time-averaged URANS. This is consistent with the total pressure and total temperature wake evolution findings noted earlier. Interestingly enough, the impact of unsteadiness is far more pronounced for the total temperature and concentration wake than the total pressure wake.

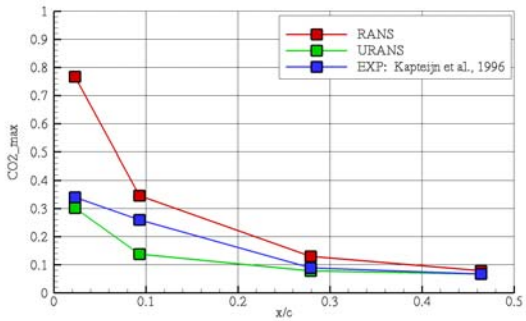

Figure 13. Maximum CO_2 concentration in wake at different moditoring locations for cm = 3% case.

5 CONCLUSIONS

Computational Fluid Dynamic simulations of a 2D transonic vane with trailing edge cooling were undertaken. Increasing the mass flow through the trailing edge slot impacted the vane loading by effectively reducing the passage shock strength. A parametric study of different turbulence models was conducted and it was noted that turbulence models had no real impact on vane loading nor on wake evolution for the baseline cm = 3% cooled case for the grid used in the investigation. Time-averaged URANS predictions resulted in more prominent wake decay rate just downstream of the coolant flow ejection location due large-scale unsteadiness. Momentum and thermal wakes evolved along different axis due to shock and viscous momentum loss mechanisms and the ejection axis of the coolant flow.

REFERENCES

[1] R. C. Wilcock, J. B. Young and J. H. Horlock, The effect of turbine blade cooling on the cycle efficiency of gas turbine power cycles, *J. Engineering for Gas Turbines and Power*, **127**, pp. 109-120 (2005)

[2] R. S. Bunker, Gas turbine heat transfer: Ten remaining hot gas path challenges, *J. Turbomachinery*, **129**, pp. 193-201 (2007)

[3] A. Roshko, On the development of turbulent wakes from vortex streets, *National Advisory Committee for Aeronautics*, Report 1191, (1954)

[4] C. H. K. Williamson, Vortex dynamics in the cyliner wake, *Annu. Rev. Fluid Mech*, **28**, pp. 477-539, (1996)

[5] P. Martini, A. Schulz, H. –J. Bauer, and C. F. Whitney, Detached eddy simulation of film cooling performance on the trailing edge cutback of gas turbine airfoils, *J Turbomachinery*, **292**, pp. 292-299 (2006)

[6] G. Medic and P. Durbin, Unsteady effects on trailing edge cooling, *J. Heat Transfer*, **127**, pp. 388-392 (2005)

[7] C. H. Sieverding and H. Heinemann, The influence of boundary layer state on vortex shedding from flat plates and turbine cascades, *J. Turbomachinery*, **112**, pp. 181-187 (1990)

[8] A. Gehrer, H. Lang, N. Mayrhofer, J. Woisetschlager, Numerical and experimental investigation of trailing edge vortex shedding downstream of a linear turbine cascade, *2000-GT-434*, (2000)

[9] G. Cicatelli and C. H. Sieverding, The effect of vortex shedding on the unsteady pressure distribution around the trailing edge of a turbine blade, *J. Turbomachinery*, **119**, pp. 810-819 (1997)

[10] C. H. Sieverding, H. Richard, and J.-M. Desse, Turbine blade trailing edge flow characteristics at high subsonic outlet Mach number, *J. Turbomachinery*, **125**, pp. 298-309, (2003)

[11] A. L. Brundage, M. W. Plesniak, P. B. Lawless and S. Ramadhyani, Experimental investigation of airfoil trailing edge heat transfer and aerodynamic losses, *Experimental Thermal and Fluid Science*, **31**, pp. 249-260 (2007)

[12] F. E. Ames, J. D. Johnson and N. J. Fiala, Gill slot trailing edge aerodynamics-effects of blowing rate, Reynolds number and external turbulence on aerodynamic losses and pressure distribution, *GT2007-27399* (2007)

[13] Y. Chen, C. G. Matalanis and J. K Eaton, High resolution PIV measurements around a model turbine blade trailing edge film cooling breakout, *Exp. Fluids*, **44**, pp. 199-209 (2008)

[14] C. Kapteijn, J. Amecke and V. Michelassi, Aerodynamic performance of a transonic turbine guide vane with trailing edge coolant ejection: Part I – Experimental approach", *J. Turbomachinery*, **118**, pp.519-528 (1996)

[15] C. H. Sieverding, T. Arts, R. Denos, and F. Martelli, Investigation of the flow field downstream of a turbine trailing edge cooled nozzle guide vane, *J. Turbomachinery*, **118**, pp. 291-300 (1996)

[16] D. C. Wilcox, Multiscale model for turbulent flows", *AIAA J.*, **26**, 1311 (1988)

[17] F. R. Menter, Two-equation eddy-viscosity turbulence models for engineering applications, *AIAA J.*, **32**(8), p. 1598-1605 (1994)

[18] P. R. Spalart and S. R. Allmaras, A one-equation turbulence model for aerodynamic flows, *AIAA Paper* 92-0439 (1992)

[19] G. Xu and Y. Zhou, Momentum and heat transfer in a turbulent cylinder wake behind a streamwise oscillating cylinder, *Int. J. of Heat and Mass Transfer*, **48**, pp. 4062-4072 (2005)

[20] W. Ning and L. He, Some modelling issues on trailinge-edge vortex shedding, *AIAA Journal*, **39**(5), pp.787-793 (2001)